European Review for Medical and Pharmacological Sciences 2018; 22: 5605-5613

MicroRNA-544 inhibits inflammatory response and cell apoptosis after cerebral ischemia reperfusion by targeting IRAK4

R. FANG[1], N.-N. ZHAO[2,3], K.-X. ZENG[4], Q. WEN[5], P. XIAO[5], X. LUO[6], X.-W. LIU[5], Y.-L. WANG[1]

[1]Department of Rehabilitation, The First Affiliated Hospital, Shenzhen University, Shenzhen Second People's Hospital, Shenzhen, China
[2]Acupuncture and Rehabilitation College, Guangzhou University of Traditional Chinese Medicine, Guangzhou, China
[3]Department of Acupuncture and Massage, Shenzhen Luohu District Hospital of Chinese Medicine, Shenzhen, China
4Department of Acupuncture and Massage, Guangdong Province Second Hospital of Traditional Chinese Medicine, Guangzhou, China
[5]Department of Rehabilitation, Shenzhen Dapneg New District Nanao People's Hospital, Shenzhen, China
[6]Department of Rehabilitation, Shenzhen Sanming Group, Kerry Rehabilitation Medicine Research Institute, Shenzhen, China

Rui Fang and *Nana Zhao* contributed equally to this work

Abstract. – OBJECTIVE: Stroke remains the most common malignant cerebrovascular event in the world. The correlation between the expression of miR-544 and the degree of cerebral ischemia reperfusion (CIR) injury has not been well recognized in recent years. This study focuses on the effect of miR-544 on inflammation and apoptosis after CIR.

PATIENTS AND METHODS: Plasma expression of miR-544 in ischemic stroke (IS) patients and healthy controls was determined by quantitative reverse transcriptase-polymerase chain reaction (qRT-PCR). The effects of miR-544 on cerebral infarction and neurological deficits were verified *in vitro* by tail vein injection of Ago-miR-544. Western blotting was utilized to examine protein expressions of key proteins involving in inflammation and apoptosis in mouse brain. Western blotting, immunofluorescence staining and luciferase assays were used to demonstrate whether miR-544 influences the expression of interleukin-1 receptor-associated kinase 4 (IRAK4), downstream inflammatory and apoptosis-related proteins.

RESULTS: MiR-544 was found decreased in peripheral blood of IS patients compared with healthy controls. MiR-544 has been shown to relieve neurological deficits and reduce the volume of cerebral infarction in mice. Overexpression of miR-544 ameliorated the inflammation and apoptotic responses in brain tissue after ischemia reperfusion by down-regulating the expression of IRAK4, whereas the low expression was opposite *in vivo* and *in vitro*.

CONCLUSIONS: We found that miR-544 may participate in controlling inflammation and apoptosis after ischemia-reperfusion by targeting IRAK4, providing possible diagnostic indicators and therapeutic targets for IS.

Key Words:
MicroRNA-544, IRAK4, Inflammatory responses, Apoptosis, CIR.

Introduction

The incidence of stroke has increased year by year globally, especially among women, becoming a serious public health problem[1-3]. CIR injury is a condition of blood perfusion recovery after a short period of ischemia and hypoxia, which aggravates brain tissue damage. It plays a significant role in the process of stroke[4,5]. Oxidative stress, apoptosis and activated inflammatory response are often known as a series of responses after CIR[6,7]. Therefore, the inhibition of oxidative stress, apoptosis and inflammatory response after CIR is of vital importance to the prognosis and

Corresponding Author: Xuanwei Liu, MM; e-mail: liuxuanwei1000@163.com; Yulong Wang, MM; e-mail: wangyulong@szu.edu.cn

treatment of stroke. MicroRNAs (miRNAs) are small RNAs with 21-25 nucleotides that partially bind to complementary sequences in the 3'-untranslated region (3'-UTR) of messenger RNA (mRNA). MicroRNAs exert their role via negatively affecting post-transcriptional regulation[8,9]. Previous studies[10,11]have found that differentially expressed miRNAs are related to the development of a wide variety of cerebrovascular diseases. For example, miRNA-125b reduces CIR injury by targeting CK2α/NADPH oxidase signaling. MiR-193 leads to toxic aldehyde accumulation and tyrosine hydroxylase dysfunction after CIR by targeting ALDH2[12,13]. MiR-544 is located in the highly conserved imprinted Dlk1-Dio3 region in mammals[14]. A series of researches have found that miR-544 is involved in the development of various diseases such as cancer, neuralgia, asthma, etc.[15-18]. However, the role of miR-544 in the progress of CIR is rarely reported.

Interleukin-1 receptor-associated kinase 4 (IRAK4) belongs to IRAK family, alongside with IRAK-1, IRAK-2 and IRAK-M[19]. IRAK4 is involved in inflammatory reactions in a variety of diseases[20,21], especially tumor immunity during tumorigenesis[22,23]. In cerebrovascular disease, IRAK4 inhibits neointimal formation in carotid arteries after balloon injury through toll like receptor 4 (TLR4)/NFκB (nuclear factor kappa-B) signaling pathway. Additionally, IRAK4 also participates in neuroinflammation through inhibition of TLR2 and TLR4 pathways in cerebral ischemia caused by middle cerebral artery occlusion[24,25]. However, it is still unknown whether IRAK4 is involved in CIR.

In this manuscript, the expression of miR-544 was first found to be lower in the peripheral blood of IS patients. MiR-544 was validated for inhibiting inflammation and apoptosis through the establishment of a mouse CIR model. Finally, it was demonstrated that miR-544 inhibits inflammation and apoptosis after CIR by targeting IRAK4.

Patients and Methods

Patient Sample Collection

50 IS (ischemic stroke) patients and 50 healthy controls who were hospitalized in Shenzhen Second People's Hospital were selected since 2017. This study was approved by the Ethics Committee of Shenzhen Second People's Hospital. Signed written informed consents were obtained from all participants before the study. The enrollment of IS patients was based on: (1) acute focal neurological deficits, (2) IS period of more than 24 hours, and (3) positive results of magnetic resonance imaging (MRI) and computed tomography (CT) in the brain. Patients with history of hemorrhagic embolism, peripheral arterial occlusion, chronic liver and kidney disease, primary or metastatic tumors or other malignant diseases were excluded. Healthy controls were also recruited during the same period. Influencing factors such as hypertension, diabetes, cardiovascular and cerebrovascular diseases were excluded through physical signs and laboratory tests. Blood samples of all participants were drawn after fasting for at least 12 hours, centrifuged at 2,500 rpm/min for 5 min, and stored in liquid nitrogen.

Animal Model

C57 mice were purchased from Vital River (Beijing, China). C57 mice were randomly divided into CIR group (n=4), Sham-operation group (n=4) and Ago-miR-544 group (n=4). Mice in CIR group received no treatment. Mice in Sham-operation group were anesthetized for surgery and did not undergo injection. Mice in Ago-miR-544 group were anesthetized and operated, followed by injection of Ago-miR-544 (Ribobio, Guangzhou, China). The CIR mouse model was constructed using suture embolization. After routine anesthesia, a midline neck incision was realized and the left common carotid artery and external carotid artery were separated and ligated. After the arteriotomy, the nylon monofilament was inserted into the left internal carotid artery and advanced cranially to the origin of the middle cerebral artery until a mild resistance was felt. The occluded filaments were maintained for 60 min. The blocked nylon fibers were then withdrawn to allow reperfusion. After 24 hours of reperfusion, each mouse was decapitated for brain tissue collection. Brain coronal sections were taken and immersed in 2% triphenyltetrazolium chloride at 37°C for 30 min. After staining, the brain samples were fixed in 4% paraformaldehyde for 24 hours. The study was approved by the Animal Ethics Committee of Shenzhen University Animal Center.

Cell Culture

BV2 cells (mouse microglia cell line) were purchased from the Academy of Sciences (Shanghai, China). Cells were cultured in Roswell Park Memorial Institute 1640 (RPMI-1640) medium (Gibco, Rockville, MD, USA) supplemented with

10% fetal bovine serum (FBS) (Gibco, Rockville, MD, USA), 100 U/mL penicillin and 100 μg/mL streptomycin (HyClone, South Logan, UT, USA) at 37°C in a 5% CO_2 humidified cell incubator. Logarithmic growth phase cells were cultured for subsequent experiments.

Cell Transfection

The mmu-miR-544-mimics, mmu-miR-544-inhibitor and NC were purchased from Ribobio (Guangzhou, China). MiR-544 mimics and NC were purchased from Gene Pharma (Shanghai, China). BV2 cells in logarithmic growth phase were taken, passaged and plated into 6-well plates (Corning, Corning, NY, USA). When the cell confluence reached 70%, transfection was performed by Lipofectamine® 3000 (Invitrogen, Carlsbad, CA, USA) according to the instructions. Cells were harvested 48 h later for follow-up experiments.

Total RNA Extraction

1 mL of TRIzol solution (Invitrogen, Carlsbad, CA, USA) was added in 100 mg of brain tissue for lysis. 2×10^5 BV2 cells were digested with trypsin, washed once with phosphate-buffered saline (PBS) solution (HyClone, South Logan, UT, USA), and lysed by adding 1 mL TRIzol solution. The total RNA was extracted with phenol chloroform. The extracted RNA was measured for purity by UV spectrophotometry and labeled. Finally, the RNA samples were stored in a -80°C freezer.

Quantitative Reverse Transcription Polymerase Chain Reaction (qRT-PCR)

Total RNA samples were thawed on ice. Reverse transcription was performed according to the instructions of the PrimeScript RT reagent (TaKaRa, Otsu, Shiga, Japan). QRT-PCR was performed using the SYBR Green Master Mix I (TaKaRa, Otsu, Shiga, Japan) on the ABI 7900 Fast Real-Time PCR System (ABI, Foster City, CA, USA). All miRNA samples were calibrated with U6 and all mRNA samples were calibrated with glyceraldehyde 3-phosphate dehydrogenase (GAPDH). The reaction conditions were set as follows: pre-denaturation at 95°C for 30 s, followed by 45 cycles of 95°C for 5 s and 60°C for 30 s per cycle. A dissolution curve was introduced. Relative quantification was performed using the $2^{-\Delta\Delta CT}$ method. For miRNAs, primer probes were designed and synthesized by Gemma (Shanghai, China). Gene primers were designed by Primer 5.0. The specific gene primer sequences were as follows: IRAK4 (F, 5'-CAAGTGATGGAGATGACCTCTGCTTAGT-3'; R, 5'-TCTAGCAATAACTGAGGTTCACGGTGTT-3'), interleukin-1 beta (IL-1β) (F, 5'-AATCTCACAGCACATCAA-3; R, 5'-AGCCCATACTTTAGGAAGACA-3'), Tumor necrosis factor (TNF)-α (F, 5'-TTCGAGTGACAAGCCTGTAGC-3'; R, 5'-AGATTGACCTCAGCGCTGAGT-3'), B-cell lymphoma-2 (Bcl-2) (F, 5'-GAACTGGGGGAGGATTGTGG-3'; R, 5'-GCATGCTGGGGCCATATAGT-3') and Bcl-2-associated X (Bax) (F, 5'-CTGGATCCAAGACCAGGGTG-3; R, 5'-CCTTTCCCCTTCCCCCATTC-3'). Each sample was detected in triplicate.

Western Blotting

0.5 M Ethylene Diamine Tetraacetic Acid (EDTA) (Beyotime, Shanghai, China), protease inhibitors (Beyotime, Shanghai, China) and phosphatase inhibitors (Beyotime, Shanghai, China) were added into the radioimmunoprecipitation assay (RIPA) solution (Beyotime, Shanghai, China) in a ratio of 100:1. 50 mg of brain tissue were selected, ground into a powder and added into the above solution. For BV2 cells, 2×10^5 cells were digested with trypsin, washed once with PBS (Gibco, Rockville, MD, USA) and added into the above solution after centrifugation. The above solution was transferred to a 1.5 mL Eppendorf (EP) tube (Corning, Corning, NY, USA). After shaking for 30 min, the EP tube was placed on a cryogenic centrifuge and centrifuged at 12000 rpm/min for 15 min at 4°C. The protein sample was added into sodium dodecyl sulphate-polyacrylamide gel electrophoresis (SDS-PAGE) protein loading buffer (Beyotime, Shanghai, China) in a 1:4 volume ratio and mixed well. The sample was then placed in boiling water for 5 min. Proteins extracted from BV2 cells and brain tissues were separated by 10% SDS-polyacrylamide gels and transferred to polyvinylidene difluoride (PVDF) membranes (Roche, Basel, Switzerland). After being blocked with 5% nonfat dry milk for 2 hours, the membrane was incubated at 4°C with the following specific primary antibodies (IRAK4 (ab13685), Bcl-2 (ab32124), Bax (ab182734), IL-1β (ab200478) and TNF-α (ab6671) (1:1000; Abcam, Cambridge, MA, USA) and GAPDH primary antibody (ab9485) (1:2000; Abcam, Cambridge, MA, USA). Membranes were then incubated with horseradish peroxidase (HRP)-conjugated anti-rabbit IgG (1:2000) for 2 hours at room temperature and then incubated 3 times with Tris-buffered saline and Tween (TBS-T) buffer

(Beyotime, Shanghai, China). The secondary antibody was detected by an enhanced chemiluminescence (ECL) system (Pierce Biotechnology, Rockford, IL, USA). The experiments were performed in triplicate.

Luciferase Reporter Assay

The 3'-UTR sequence or mutated sequence of IRAK4 was inserted into the pLG3 promoter vector (Promega, Madison, WI, USA), respectively for constructing pLG3-IRAK4-WT and pLG3-IRAK4-MuT. BV2 cells were seeded in 6-well plates (Corning, Corning, NY, USA) and transfected with 100 ng of pLG3-IRAk4-WT or pLG3-IRAK4-MuT, miR-544 mimics and NC with Lipofectamine 3000 (Invitrogen, Carlsbad, CA, USA), respectively. After 48 hours, transfected cells were collected for detecting relative luciferase activity using the Luciferase Assay Kit (Promega, Madison, WI, USA).

Immunofluorescence Staining Assay

Brain sections were fixed with 4% paraformaldehyde for 30 min at 37°C and then blocked and permeabilized for 1 hour at room temperature with buffer A. Anti-IRAK4 (1:500, ab13685) was added and incubated overnight at 4°C. Brain sections were conjugated to Alexa Fluor 594 donkey anti-rabbit (1:1000, A21207, Invitrogen, Carlsbad, CA, USA). The diabodies were incubated for 2 hours at room temperature. DAPI (4',6-diamidino-2-phenylindole) staining solution (Thermo Fisher Scientific, Waltham, MA, USA) was used to label the nucleus. The image was captured by a ZEISS microscope (Oberkochen, Germany).

Statistical Analysis

All experimental data were analyzed using GraphPad software 6.0 (La Jolla, CA, USA) and Statistical Product and Service Solutions (SPSS) 18.0 for statistical analysis (SPSS Inc., Chicago, IL, USA). The *p*-values were analyzed using Student's *t*-test, one-way ANOVA and Spearman's test. $p < 0.05$ was considered statistically significant.

Results

The Level of miR-544 in IS Patients and CIR Mouse Brain is Significantly Reduced

Plasma expression of miR-544 was measured by qRT-PCR. The data showed that plasma expression of miR-544 of IS patients is significantly lower than that of the control group (Figure 1A). An *in vivo* experiment was performed to verify this phenomenon again (Figure 1B). MiR-544 expression in brain tissues of CIR mice was significantly decreased compared with those of Sham-operation group (Figure 1C). In addition, miR-544 expression was significantly enhanced by tail vein injection of Ago-miR-544 compared with those of the CIR group (Figure 1D). The above results indicated that miR-544 may be involved in the process of CIR.

MiR-544 Alleviates Neurological Deficits and Reduces Cerebral Infarction Volume in Mice

Zea-Longa 5-point scheme was used to evaluate the neurological deficits in mice. Three groups of mice were scored at 24, 48 and 72 h after reperfusion, respectively. It was worth noting that, at 24 and 48 h, the score of Ago-miR-544 group was significantly lower than that of CIR group (Figure 2A), while Sham-operation group score was always 0, indicating no neurological deficits at the three time points. To verify the effect of miR-544 on cerebral infarction, brain tissues were stained with triphenyltetrazolium chloride (Figure 1B). The results showed that there was no staining in Sham-operation group, while a pale infarct area was seen in the CIR and Ago-miR-544 groups. Moreover, the pale volume in CIR group was significantly larger than that of Ago-miR-544 group (Figure 2B). The results indicated that miR-544 alleviates neurological deficits and reduces cerebral infarction volume in mice.

MiR-544 Inhibits Inflammatory Responses and Apoptosis After CIR

In order to detect inflammation and apoptosis after CIR, Western blotting was used to detect the protein levels of IL-1β, TNF-α, Bax and Bcl-2. As shown in Figure 3A and 3B, compared with CIR group, protein expressions of IL-1β, TNF-α, and Bax in Ago-miR-544 group was significantly decreased, while Bcl-2 expression level was significantly increased. At the same time, mRNA expressions of the abovementioned genes were measured by qRT-PCR. Compared with CIR group, mRNA expressions of IL-1β, TNF-α and Bax were significantly decreased in Ago-miR-544 group, while the expression level of Bcl-2 was significantly increased (Figure 3C). These results indicated that miR-544 suppresses the inflammatory response and reduces the degree of apoptosis after CIR.

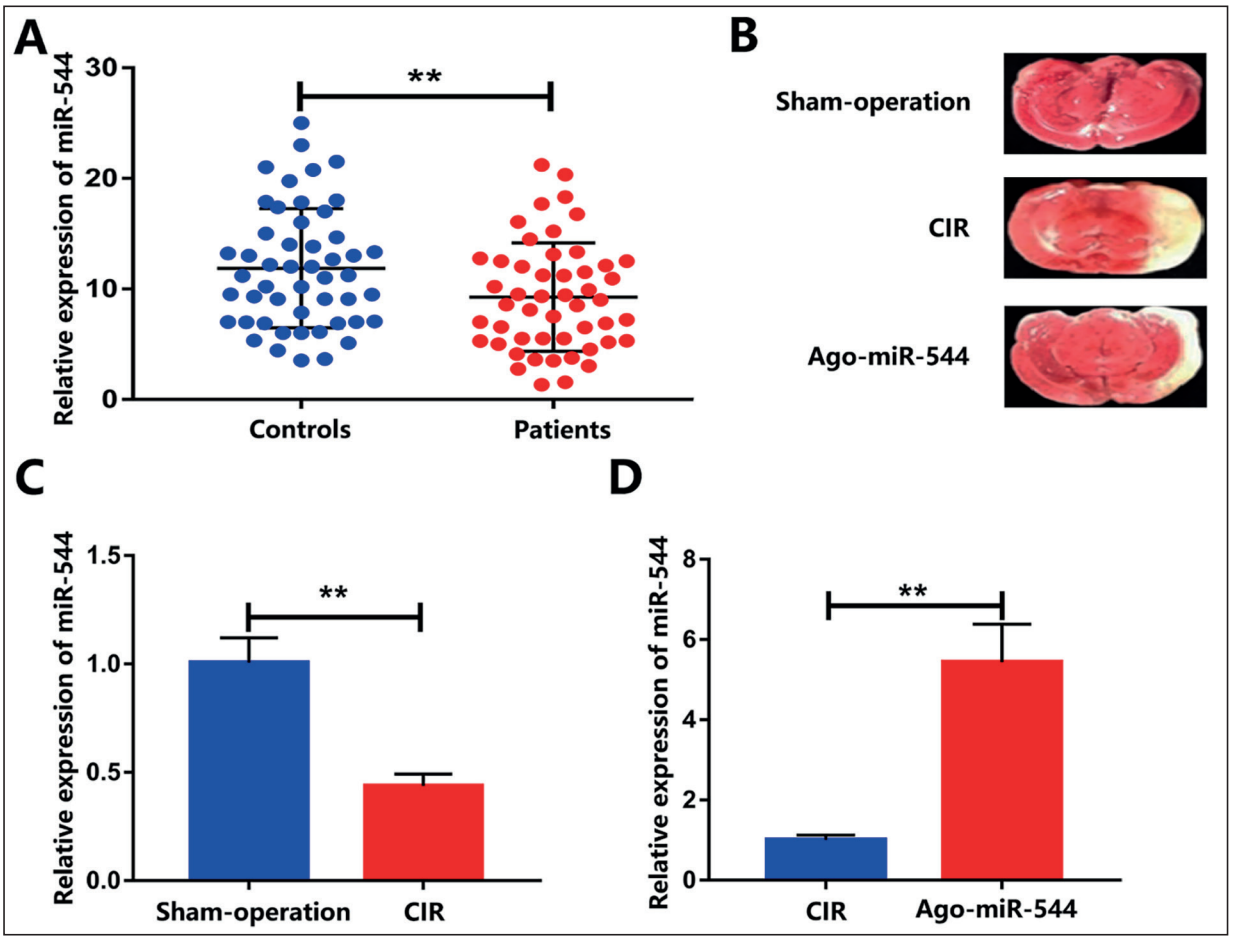

Figure 1. The level of miR-544 in IS patients and CIR mouse brain. ***A,*** The expression of miR-544 in peripheral blood of IS patients and healthy controls. ***B,*** Brain tissue sections and staining were performed in each group of mice. ***C,*** The level of miR-544 in brain tissues in CIR group and Sham-operation group. ***D,*** Expression of miR-544 in the group injected with Ago-miR-544 vial caudal vein compared with that of CIR group. Data were presented as the mean ± SD of three independent experiments (*$p < 0.05$, **$p < 0.01$).

MiR-544 Inhibits IRAK4 Expression by Interacting Directly with the Putative Binding Site of IRAK4-3'-UTR

Previous studies[26] have shown that miRNAs interact with the target genes *via* the 3' UTR. The potential targets for miR-544 were searched from MicroRNA.org, MiRWalk and TargetScan and IRKA4 was found to be a potential target for miR-544. The predicted binding site for miR-544 and IRAK4 was shown in Figure 4A. Luciferase activity assay was performed to further verify the binding of miR-544 and IRAK4. The wild-type (WT) and mutant-type (MuT) sequences of IRAK4 were inserted into the luciferase reporter vector. Then, the pGL3 luciferase reporter vector and miR-544 mimics or NC were co-transfected into BV2 cells. After 48 hours, the luciferase activity of WT group was significantly lower than that of MuT group (Figure 4B). These above results indicated that IRAK4 is a potential target of miR-544.

Overexpression of miR-544 Inhibits Inflammation and Apoptosis by Targeting IRAK4

IRAK expression in Ago-miR-544 group was significantly reduced compared to the CIR group through tissue immunofluorescence staining assay (Figure 5A). In addition, it was confirmed that IRAK4 expression in Ago-miR-544 group was significantly decreased by Western blotting (Figure 5B). To further verify the downregulation of IRAK4 by miR-544, mmu-miR-544-mimics, mmu-miR-544-inhibitor or NC was transfected into BV2 cells and the transfection efficiency was verified (Figure 5C and 5D). As shown in

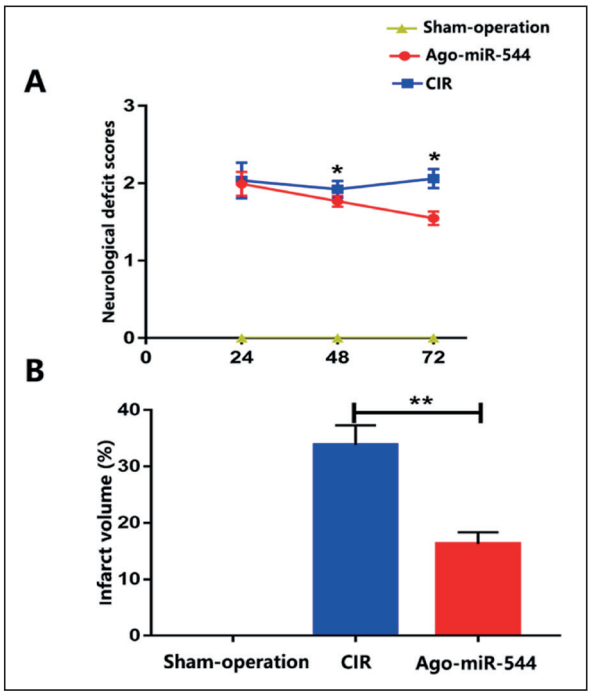

Figure 2. Effect of Ago-miR-544 on neurological deficits and cerebral infarction volume of mice with CIR. ***A***, Neurological deficit scores were determined according to Zea-Longa 5-point scheme in three groups. ***B***, Brain tissues were stained using triphenyl tetrazolium chloride and the volume of infarction was measured. Data were presented as the mean ± SD of three independent experiments (*$p < 0.05$, **$p < 0.01$).

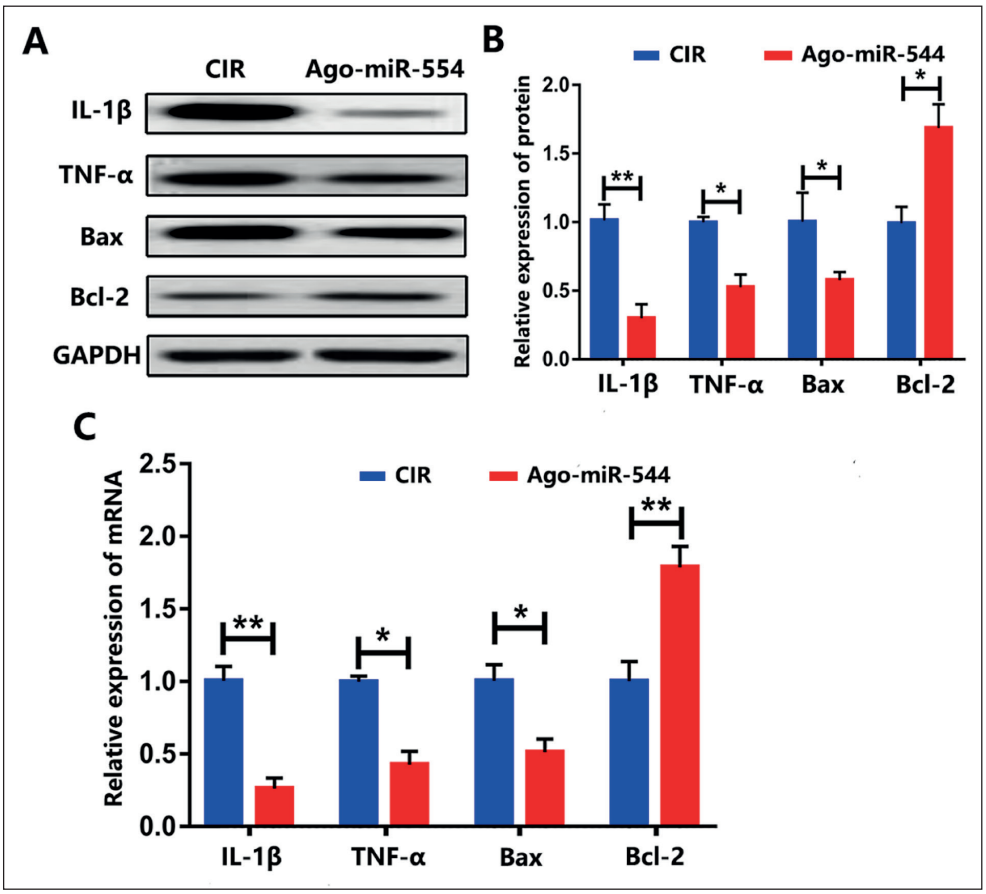

Figure 3. Effect of Ago-miR-544 on inflammatory responses and cell apoptosis after CIR. Protein (***A*** and ***B***) and mRNA (***C***) levels of IL-1β, TNF-α, Bax and Bcl-2 proteins were determined by Western blotting and qPCR, respectively. Data were presented as the mean ± SD of three independent experiments (*$p < 0.05$, **$p < 0.01$).

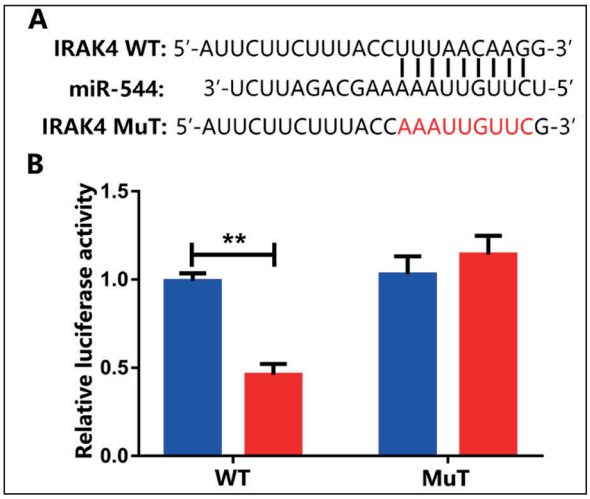

Figure 4. IRAK4 is a possible target for miR-544. ***A,*** Possible binding sites between IRAK4 and miR-544. ***B,*** The fluorescence intensity of the WT group was significantly weaker than that of the MuT group. Data were presented as the mean ± SD of three independent experiments (*$p < 0.05$, **$p < 0.01$).

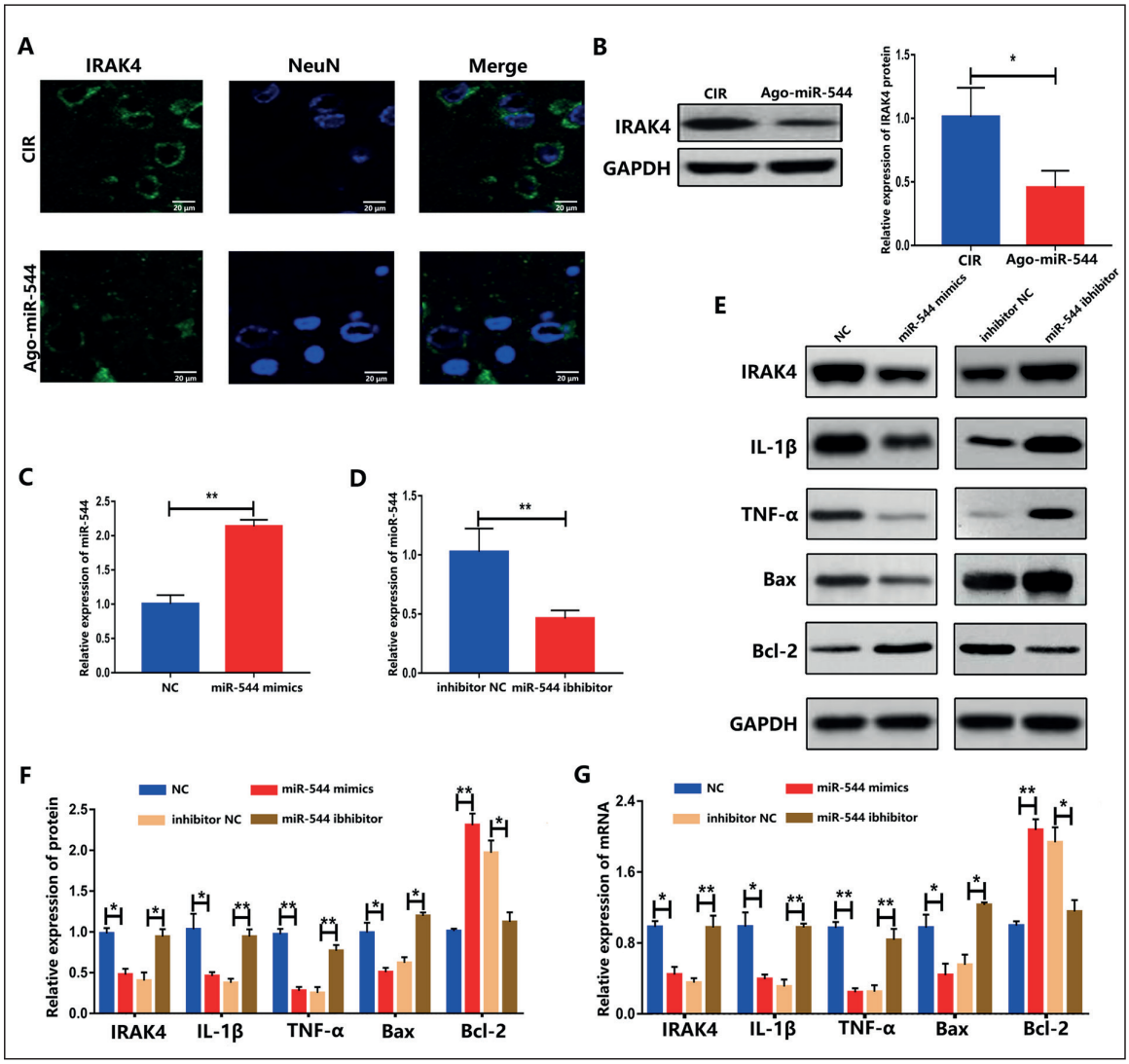

Figure 5. Overexpression of miR-544 inhibits inflammation and apoptosis by targeting IRAK4. ***A,*** The immunofluorescence of IRAK4 in mouse brain tissue. ***B,*** IRAK4 protein expression in mouse brain (50×). ***C,*** and ***D,*** Expression of miR-544 after transfection. ***E-G,*** After overexpression of miR-544, the expression of IRAK4, inflammatory and apoptotic proteins decreased. Data were presented as the mean ± SD of three independent experiments (*$p < 0.05$, **$p < 0.01$).

Figure 5E, 5F and 5G, overexpression of miR-544 significantly reduced the expressions of IRAK4, IL-1β, TNF-α and Bax, and enhanced the expression of Bcl-2 by qRT-PCR. At the same time, knockdown of miR-544 increased the expressions of IRAK4, IL-1β, TNF-α and Bax and decreased the expression of Bcl-2. These results indicated that miR-544 could alleviate inflammation and apoptosis after CIR by targeting IRAK4.

Discussion

In our current study, miR-544 was first found to be lowly expressed in the peripheral blood of IS patients. Overexpression of miR-544 reduced cerebral neurological deficits and decreased cerebral infarction volume in mice. It was found that inflammation and apoptosis in mouse brain tissue samples were significantly reduced in Ago-miR-544 group compared with those CIR group. In addition, miR-544 was shown to regulate IRAK4 expression by Western blotting, immunofluorescence staining and luciferase assay, respectively. Therefore, these observations indicated that miR-544 alleviates inflammation and apoptosis by targeting IRAK4 after CIR, which could be used as a diagnostic and therapeutic indicator of ischemic stroke.

MiR-544, a member of the miRNA family, was first reported to play a role in guiding prognosis in esophageal cancer[27]. In a mouse model, miR-544 has also been shown to relieve neuralgia by targeting STAT3[15]. However, the role of miR-544 in CIR has not been studied. The TLR/IL-1R family plays a regulatory role in various immune responses, among which IRAK4 is a key factor in the signal transduction system of the TLR/IL-1R family[28]. TIR family receptors are activated at the onset of inflammation and promote the binding of IRAK4 and IRAK1. IRAK1 is then phosphorylated by IRAK4, and phosphorylated IRAK1 initiates autophosphorylation of IRAK1, which ultimately results in hyperphosphorylated IRAK1. Alteration of IRAK1 ligand results in activation of NF-κB. As a result, activated NF-κB stimulates the activation of pro-inflammatory cytokines IL-1β, IL-6 and TNF-α, and induces downstream cascades of inflammatory responses, leading to tissue inflammatory lesions and apoptotic cell responses[29-31].

However, there are some limitations in this research. IRAK4 is just one of many potential targets of miR-544. In this study, we only confirmed that miR-544 alleviates the progression of inflammation and apoptosis by targeting IRAK4. Whether there are other mechanisms still needs further discussion. This work confirmed that miR-544 may play a key role in the regulation of inflammation and apoptosis by downregulating IRAK4. Overexpression of miR-544 may be a potential method for relieving CIR injury.

Conclusions

We showed that miR-544 has an inhibitory effect on inflammation and apoptosis after CIR *in vitro* and *in vivo*. In addition, miR-544 inhibits the progression of inflammation and apoptosis by inhibiting IRAK4. Our results indicate that miR-544 could be used as a diagnostic indicator for ischemic stroke.

Acknowledgements

This study was supported by Shenzhen "Sanming Project" (SZSM201610039).

Conflict of Interest

The Authors declare that they have no conflict of interests.

References

1) Hennerici MG. Synergistic strategies to promote stroke research. Cerebrovasc Dis 2018; 45: I-II.
2) Rosenberg K. Stroke risk factors unique to women. Am J Nurs 2018; 118: 69-70.
3) Niewada M, Kobayashi A, Sandercock PA, Kaminski B, Czlonkowska A. Influence of gender on baseline features and clinical outcomes among 17,370 patients with confirmed ischaemic stroke in the international stroke trial. Neuroepidemiology 2005; 24: 123-128.
4) Zhao JJ, Xiao H, Zhao WB, Zhang XP, Xiang Y, Ye ZJ, Mo MM, Peng XT, Wei L. Remote ischemic postconditioning for ischemic stroke: a systematic review and meta-analysis of randomized controlled trials. Chin Med J (Engl) 2018; 131: 956-965.
5) Hu YQ, Chen W, Yan MH, Lai JJ, Tang N, Wu L. Ischemic preconditioning protects brain from ischemia/reperfusion injury by attenuating endoplasmic reticulum stress-induced apoptosis through PERK pathway. Eur Rev Med Pharmacol Sci 2017; 21: 5736-5744.
6) Wu MY, Yiang GT, Liao WT, Tsai AP, Cheng YL, Cheng PW, Li CY, Li CJ. Current mechanistic concepts in ischemia and reperfusion injury. Cell Physiol Biochem 2018; 46: 1650-1667.

7) Melek FE, Baroncini LA, Repka JC, Nascimento CS, Precoma DB. Oxidative stress and inflammatory response increase during coronary artery bypass grafting with extracorporeal circulation. Rev Bras Cir Cardiovasc 2012; 27: 61-65.

8) Kim J, Yao F, Xiao Z, Sun Y, Ma L. MicroRNAs and metastasis: small RNAs play big roles. Cancer Metastasis Rev 2018; 37: 5-15.

9) Pasquinelli AE. MicroRNAs and their targets: recognition, regulation and an emerging reciprocal relationship. Nat Rev Genet 2012; 13: 271-282.

10) Wang J, Zhang Y, Xu F. Function and mechanism of microRNA-210 in acute cerebral infarction. Exp Ther Med 2018; 15: 1263-1268.

11) Hromadnikova I, Kotlabova K, Ivankova K, Vedmetskaya Y, Krofta L. Profiling of cardiovascular and cerebrovascular disease associated microRNA expression in umbilical cord blood in gestational hypertension, preeclampsia and fetal growth restriction. Int J Cardiol 2017; 249: 402-409.

12) Liang Y, Xu J, Wang Y, Tang JY, Yang SL, Xiang HG, Wu SX, Li XJ. Inhibition of MiRNA-125b decreases cerebral ischemia/reperfusion injury by targeting CK2alpha/NADPH oxidase signaling. Cell Physiol Biochem 2018; 45: 1818-1826.

13) Mao L, Zuo ML, Hu GH, Duan XM, Yang ZB. Mir-193 targets ALDH2 and contributes to toxic aldehyde accumulation and tyrosine hydroxylase dysfunction in cerebral ischemia/reperfusion injury. Oncotarget 2017; 8: 99681-99692.

14) Cao C, Wen Y, Dong J, Wang X, Qin W, Huang X, Yuan S. Maternally expressed miR-379/miR-544 cluster is dispensable for testicular development and spermatogenesis in mice. Mol Reprod Dev 2018; 85: 175-177.

15) Jin H, Du XJ, Zhao Y, Xia DL. XIST/miR-544 axis induces neuropathic pain by activating STAT3 in a rat model. J Cell Physiol 2018; 233: 5847-5855.

16) Haga CL, Velagapudi SP, Strivelli JR, Yang WY, Disney MD, Phinney DG. Small molecule inhibition of miR-544 biogenesis disrupts adaptive responses to hypoxia by modulating ATM-mTOR signaling. Acs Chem Biol 2015; 10: 2267-2276.

17) Qiu YY, Zhang YW, Qian XF, Bian T. MiR-371, miR-138, miR-544, miR-145, and miR-214 could modulate Th1/Th2 balance in asthma through the combinatorial regulation of Runx3. Am J Transl Res 2017; 9: 3184-3199.

18) Sarver AL, Thayanithy V, Scott MC, Cleton-Jansen AM, Hogendoorn PC, Modiano JF, Subramanian S. MicroRNAs at the human 14q32 locus have prognostic significance in osteosarcoma. Orphanet J Rare Dis 2013; 8: 7.

19) Akira S, Takeda K. Toll-like receptor signalling. Nat Rev Immunol 2004; 4: 499-511.

20) Pasterkamp G, Van Keulen JK, De Kleijn DP. Role of Toll-like receptor 4 in the initiation and progression of atherosclerotic disease. Eur J Clin Invest 2004; 34: 328-334.

21) Arroyo-Espliguero R, Avanzas P, Jeffery S, Kaski JC. CD14 and toll-like receptor 4: a link between infection and acute coronary events? Heart 2004; 90: 983-988.

22) Cheng BY, Lau EY, Leung HW, Leung CO, Ho NP, Gurung S, Cheng LK, Lin CH, Lo RC, Ma S, Ng IO, Lee TK. IRAK1 augments cancer stemness and drug resistance via the AP-1/AKR1B10 signaling cascade in hepatocellular carcinoma. Cancer Res 2018; 78: 2332-2342.

23) Zhang D, Li L, Jiang H, Li Q, Wang-Gillam A, Yu J, Head R, Liu J, Ruzinova MB, Lim KH. Tumor-Stroma IL1beta-IRAK4 feed forward circuitry drives tumor fibrosis, chemoresistance, and poor prognosis in pancreatic cancer. Cancer Res 2018; 78: 1700-1712.

24) Bai S, Li D, Zhou Z, Cao J, Xu T, Zhang X, Wang Y, Guo J, Zhang Y. Interleukin-1 receptor-associated kinase 1/4 as a novel target for inhibiting neointimal formation after carotid balloon injury. J Atheroscler Thromb 2015; 22: 1317-1337.

25) Wang Y, Ge P, Yang L, Wu C, Zha H, Luo T, Zhu Y. Protection of ischemic post conditioning against transient focal ischemia-induced brain damage is associated with inhibition of neuroinflammation via modulation of TLR2 and TLR4 pathways. J Neuroinflammation 2014; 11: 15.

26) He L, Hannon GJ. MicroRNAs: small RNAs with a big role in gene regulation. Nat Rev Genet 2004; 5: 522-531.

27) Sarver AL, Thayanithy V, Scott MC, Cleton-Jansen AM, Hogendoorn PC, Modiano JF, Subramanian S. MicroRNAs at the human 14q32 locus have prognostic significance in osteosarcoma. Orphanet J Rare Dis 2013; 8: 7.

28) Loiarro M, Ruggiero V, Sette C. Targeting TLR/IL-1R signalling in human diseases. Mediators Inflamm 2010; 2010: 674363.

29) Kissner TL, Moisan L, Mann E, Alam S, Ruthel G, Ulrich RG, Rebek M, Rebek JJ, Saikh KU. A small molecule that mimics the bb-loop in the toll interleukin-1 (il-1) receptor domain of myd88 attenuates staphylococcal enterotoxin b-induced pro-inflammatory cytokine production and toxicity in mice. J Biol Chem 2011; 286: 31385-31396.

30) Novikova L, Czymmeck N, Deuretzbacher A, Buck F, Richter K, Weber AN, Aepfelbacher M, Ruckdeschel K. Cell death triggered by Yersinia enterocolitica identifies processing of the proinflammatory signal adapter MyD88 as a general event in the execution of apoptosis. J Immunol 2014; 192: 1209-1219.

31) Pan J, Zhang J, Hill A, Lapan P, Berasi S, Bates B, Miller C, Haney S. A kinome-wide siRNA screen identifies multiple roles for protein kinases in hypoxic stress adaptation, including roles for IRAK4 and GAK in protection against apoptosis in VHL-/- renal carcinoma cells, despite activation of the NF-kappaB pathway. J Biomol Screen 2013; 18: 782-796.